ACS POLYMERS Au
AN OPEN ACCESS JOURNAL OF THE AMERICAN CHEMICAL SOCIETY

pubs.acs.org/polymerau
Article

Microwave-Assisted, Solid-State Procedure to Covalently Conjugate Hyaluronic Acid to Curcumin: Validation of a Green Synthetic Protocol

Valentina Verdoliva, Giuliana Muzio, Riccardo Autelli, Michele Saviano, Emiliano Bedini, and Stefania De Luca*

Cite This: ACS Polym. Au 2024, 4, 214−221
Read Online

ACCESS | Metrics & More | Article Recommendations | Supporting Information

ABSTRACT: A microwave-assisted esterification reaction to prepare hyaluronan−curcumin derivatives by employing a solvent-free process was developed. In particular, a solid-state strategy to react two molecules characterized by totally different solubility profiles was developed. Hyaluronic acid, a highly hydrosoluble polysaccharide, was reacted with hydrophobic and even water-unstable curcumin. Microwave (MW) irradiation was employed to activate the reaction between the two solid compounds through the direct interaction with them and to preserve the integrity of the sensitive curcumin species. This new protocol can be considered efficient, fast, and also eco-friendly, avoiding the employment of toxic organic bases and solvents. A cytotoxicity test suggested that the developed hyaluronan−curcumin conjugate (HA-CUR) could be considered a candidate for its implementation as a new material. In addition, preliminary studies revealed promising anti-inflammatory activity and open future perspectives of further investigation.

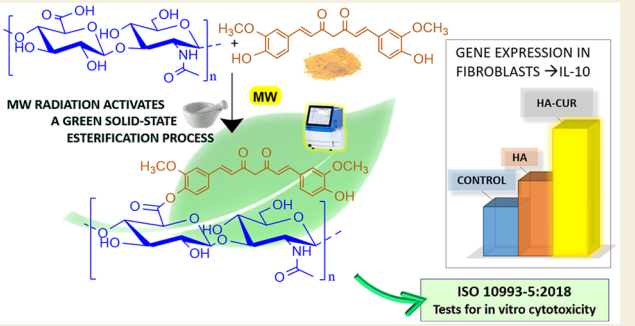

KEYWORDS: *hyaluronan−curcumin conjugate, solvent-free protocol, solid-state reaction, MW irradiation, anti-inflammatory activity*

INTRODUCTION

The success of organic reactions under the conventional solution strategy generally relies on the use of the appropriate solvent to dissolve all reactants. Indeed, it ensures the highest probability of reactant collisions with the correct orientation so that a complete and desired chemical transformation is addressed. On the other hand, following green guide lines to evaluate the environmental impact of chemical processes, it was found that solvents are the major contributors to the production of massive and undesirable waste.[1−4]

In previous studies, we performed the reaction between hydrophilic natural polymers, such as polysaccharides, and hydrophobic molecules, such as natural fatty acids.[5] In other words, we faced the problem of reacting two compounds characterized by quite different solubilities. In consequence of this, the synthetic strategy seemed very challenging and, finally, not accessible in common organic solvents (DMF, *N*,*N*-dimethylformamide; THF, tetrahydrofuran; etc.). The only solvent that could solubilize both the polysaccharide and the fatty acids was pyridine, a polar, basic, low-reactive, excellent solvent system able to solubilize a huge range of compounds. Unfortunately, pyridine is far from being a benign solvent due to its high degree of toxicity. In the end, the ideal approach turned out to be performing the conjugation reaction in the absence of any solvent, which means in the solid state, since all the employed reactants were solid and a solvent-independent strategy was developed.[6,7]

Curcumin (CUR), the yellowish polyphenolic main component of turmeric rhizomes, offers outstanding medicinal properties including anticancer, antioxidant, antimicrobial, antiamyloid, and anti-inflammatory activities, among others.[8−13] Indeed, it has drawn massive interest in research devoted to investigating its biological and pharmacological activities. The main hurdle of using CUR for treatment of diseases is its poor solubility and lack of stability in aqueous medium, in particular in basic−neutral conditions,[14−16] so that several attempts have been made to enhance its bioavailability in the bloodstream. For instance, CUR has been encapsulated in the inner core of carriers, such as chitosan, hyaluronan, poly(lactic-*co*-glycol acid), and so on,[17−22] and chemically conjugated to natural polysaccharides in order to develop amphiphilic nanocarriers of CUR.[23−29] Hyaluronic acid (HA), as a hydrosoluble polysaccharide, increases the solubility and

Received: November 28, 2023
Revised: January 23, 2024
Accepted: January 24, 2024
Published: March 20, 2024

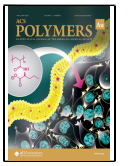

https://doi.org/10.1021/acspolymersau.3c00047
ACS Polym. Au 2024, 4, 214−221

bioavailability of CUR, while providing its own additional biological benefits (antimicrobial, anti-inflammatory, antioxidant, wound-repairing effects).[30−34]

The present paper focuses on the hypothesis that an innovative synthetic strategy could be developed for the preparation of hyaluronic acid−curcumin conjugates (HA-CUR) following a totally solvent-free protocol. The amphiphilic conjugates were prepared by performing a solid-state mechanically assisted synthesis and using microwaves for the activation. All reaction steps were performed in the absence of any solvent; in particular, the activation of the carboxylic groups present on the biomacromolecule is successfully performed either in the presence or absence of an organic or inorganic base. Consequently, the whole synthetic process becomes more valuable from an environmental, health, and safety perspective. The structural features of the obtained amphiphilic conjugates were evaluated by using UV−vis (ultraviolet−visible), fluorescence, FT-IR (Fourier transform infrared), and NMR (nuclear magnetic resonance) spectroscopy. In addition, they were finally studied for their biocompatibility with an *in vitro* test on cultured human normal fibroblasts HFF-1 (human foreskin fibroblasts). Preliminary studies to evaluate the effect on the expression of factors regulating the inflammation process were also performed on the same cell line.

MATERIALS AND METHODS

Materials

HA sodium salt from *Streptococcus equi* (15−30 kDa molecular weight), CUR, all reagents and solvents for the synthesis, and dimethyl sulfoxide (DMSO) 3-(4,5-dimethylthiazol-2yl)-2,5-diphenyltetrazolium bromide (MTT) for biological assays were purchased from Sigma−Aldrich.

Synthetic Procedures and Characterization of HA-CUR Conjugates

Synthesis of HA-CUR Conjugates. By using an agate mortar, 10 mg of HA and 10 μL of *N,N′*-diisopropylcarbodiimide (DIC) were manually milled in the presence (<1 mg-ND) of 4-(dimethylamino)-pyridine (DMAP) (Route 1) or potassium carbonate (K_2CO_3) (∼3 mg) (Route 2) or in the absence of any base (Route 3) under a fume cupboard. The mixtures, placed in a 0.5−2 mL microwave vial, were irradiated for 2 min at 80 °C in a microwave oven (Biotage Initiator+, Sweden AB, Uppsala, Sweden). In a subsequent step, by using an agate mortar, the resulting activated HA samples and 5.0 mg of CUR were manually milled in the presence of ∼3 mg of K_2CO_3 to obtain HA-CUR conjugates. The samples, placed in a 0.5−2.2 mL microwave vial, were irradiated for 2 min at 80 °C in a microwave oven. After cooling at room temperature, the obtained solid was dissolved in aqueous 0.1 M HCl (∼20 mL) in order to keep the pH at a value of 1−2 and in the absence of light. Then, it was placed in a 250 mL separatory funnel and was extracted with ethyl acetate in order to remove the unreacted CUR. During the extraction step, we monitored the pH of the aqueous solution and corrected it, if necessary, at a value of 1−2. Subsequently, the aqueous layer was dialyzed (Spectra/Por membrane cutoff of 6000−8000) in an acid aqueous solution (pH = 1−2) for 6 h, and the pH was constantly monitored. The final product was collected after the lyophilization process. Mass yield: around 40%.

Nuclear Magnetic Resonance (^{1}H NMR) Characterization. ^{1}H NMR and 1D-DOSY liquid-state NMR spectra were recorded in D_2O, DMSO-d_6, or 3:2 v/v DMSO-d_6−D_2O at 298 K on a Bruker Avance III HD 600 MHz spectrometer (Billerica, MA) equipped with a cryo-probe (^{1}H: 600 MHz, acetone as an internal standard at 2.22 ppm for spectra in D_2O, $CHD_2SO_2CD_3$ as an internal standard at 2.49 ppm for spectra in DMSO-d_6 and in 3:2 v/v DMSO-d_6−D_2O), using Bruker TopSpin 4.0.5 software. In particular, 1D-DOSY experiments were performed using a stimulated echo sequence with bipolar gradient pulses and one spoil gradient (stebpgp1s1d) with a diffusion time Δ of 300 ms and a gradient duration of 1.25 ms.

FT-IR Characterization. The derivatized HA samples were analyzed with FT-IR spectroscopy using the ATR accessory of the JASCO FT/IR-4100 Fourier transform infrared spectrometer instrument. IR transmission spectra were recorded with a number of scans of 16 at a resolution of 4 cm^{-1} over a wavenumber region of 400−4000 cm^{-1}. The relevant bands of the HA-CUR conjugates are 3428 cm^{-1} (O−H), 1732 cm^{-1} (C═O CUR ester), 1636 cm^{-1} (COO^-), 1413 cm^{-1} (COO^-), and 1078 and 1040 cm^{-1} (COC glycosidic bond ring and curcumin aromatic C−H vibrations).

UV−vis Characterization. CUR and HA-CUR conjugates were characterized with UV−vis spectroscopy using a JASCO V-730 spectrophotometer_ETCS-761 instrument. The absorbance of CUR and HA-CUR conjugates was measured in a 3:2 v/v EtOH−H_2O mixture ($C_{HA\text{-}CUR}$ = 1 mg/10 mL); spectra were recorded in the range of 250−600 nm at room temperature using 500 μL quartz cells and were corrected for blank. Other experimental settings were fixed as follows: scan speed, 200 nm/min; data interval, 0.2 nm; response, 0.24 s; data interval, 0.2 nm; scan mode, continuous; and bandwidth, 1.0 nm. The extinction coefficient of CUR in EtOH (ethanol) is 51,818 M^{-1} cm^{-1} at its absorbance maximum (λ_{max} = 432 nm).[35]

Fluorescence Spectroscopy Characterization. Fluorescence spectra were recorded at room temperature using a JASCO FP-8350 ETC-115 instrument equipped with a 1.0 cm quartz cell, with an excitation wavelength of 430 nm and an emission range of 440−650 nm. In a typical experiment, small aliquots of HA-CUR conjugates were dissolved in a 3:2 v/v EtOH−H_2O mixture ($C_{HA\text{-}CUR}$ = 1 mg/10 mL). Final spectra were obtained after a blank correction. Other experimental settings were fixed as follows: scan speed of 200 nm/min; data interval of 0.5 nm; and sensitivity: medium.

Viability Assay. Three samples of HA-CUR conjugates (A−C), prepared via route 2 (see Scheme 1), were tested for their biocompatibility. CUR and HA were also employed to evaluate the effect of the individual components of the conjugate. CUR was dissolved in dimethyl sulfoxide (highest DMSO final concentration of 0.55%). This stock solution was used to evaluate the effect of CUR at the concentration of 2 μg/mL (corresponding to the concentration found for the CUR in the HA-CUR conjugate) in 96-well plates. Cells were also exposed to 0.55% DMSO alone. HA and HA-CUR samples were dissolved in the culture medium to prepare 0.2 mg/mL stock solutions (sterilized for 1 h under UV in a sterile vertical laminar air flow cabinet). From these, several diluted solutions were prepared to treat cells at the concentrations of 5, 25, 50, and 100 μg/mL.

A test of direct cytotoxicity following the ISO 10993-5:2018 protocol was carried out using the human fibroblast cell line HFF-1 (ATCC, Rockville, MD, USA). Cells were routinely cultured in high-glucose DMEM (Dulbecco's modified Eagle medium) supplemented with 2 mM glutamine, 1% antibiotic/antimycotic solution, 1% nonessential amino acids, and 10% fetal bovine serum (FBS, v/v) and maintained in an atmosphere of 5% CO_2 and 95% air at 37 °C.

For viability analysis, cells were seeded (13,550/cm^2) in 96-well plates in 100 μL of culture medium. 24 h after seeding, DMSO, CUR, HA, and HA-CUR conjugates at different concentrations were added in order to reach the concentrations reported in Figure 5 in a final volume of 200 μL. Each sample was tested in quadruplicate. Untreated cells were used as a control.

At the different experimental times (24, 48, and 96 h), cell viability was determined by MTT assay directly on attached cells. Briefly, 20 μL of MTT (10 mg/mL) in PBS solution was added to each well and incubated for 3 h at 37 °C in a humidified atmosphere of 5% CO_2 in air. Then, the culture medium was removed and 100 μL of DMSO was added to each well to dissolve formazan precipitates that form in living cells via the activity of dehydrogenases in the mitochondria.

After 30 min of incubation at room temperature, the absorbance was measured at 595 nm by using a microplate reader (Bio-Rad Laboratories, Segrate, Italy). The absorbance of each sample was

https://doi.org/10.1021/acspolymersau.3c00047
ACS Polym. Au 2024, 4, 214−221

Scheme 1. Synthetic Strategy to HA-CUR Conjugates. Panel A: Activation Step with DMAP (Route 1), K_2CO_3 (Route 2), or Without Any Base (Route 3). Panel B: Esterification Reaction

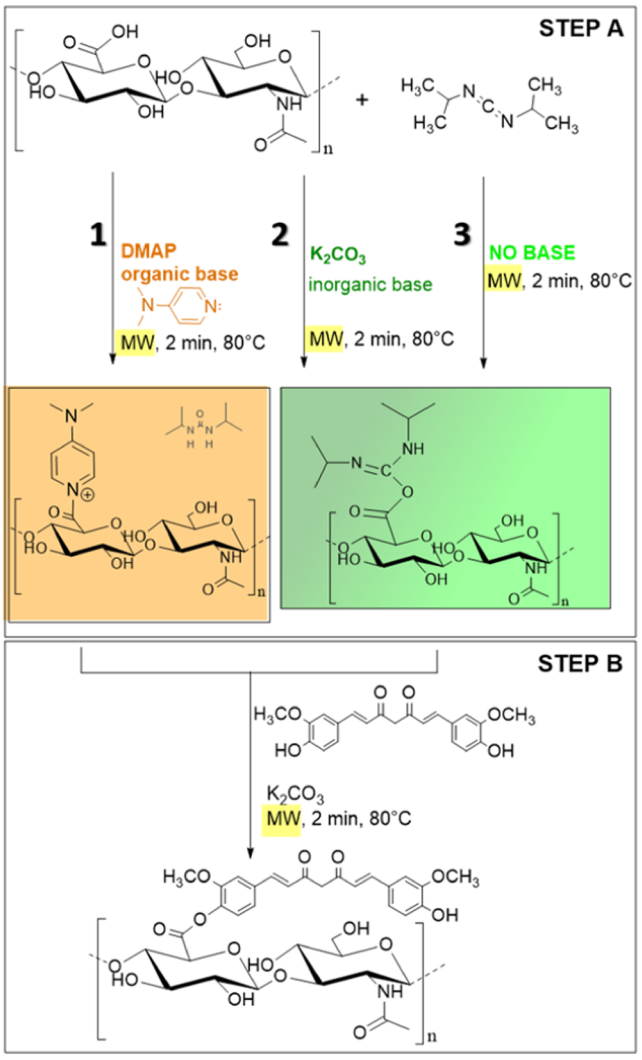

expressed as a percentage of the absorbance of the control cells at the corresponding experimental time.

Gene Expression. The human fibroblasts HFF-1 were used for IL-10 gene expression evaluation by real-time RT-PCR. The cells were exposed to HA or to the HA-CUR conjugate at the concentration of 100 μg/mL for 96 h. Then, they were collected by centrifugation at 600*g* for 10 min and stored at −80 °C until use.

Total RNA was extracted using TRIReagent (Merck Life Science, Milan, Italy). For each sample, 2.5 μg of total RNA was reverse-transcribed to cDNA using the FIREScript RT cDNA synthesis kit (Solis Biodyne, Tartu, Estonia).

Real-time PCR was performed on a volume of cDNA corresponding to 50 ng of starting RNA using 5 x HOT FIREPol Evagreen qPCR Supermix (Solis Biodyne, Tartu, Estonia). The forward (F) and reverse (R) primers were either downloaded from the Primer Bank (https://pga.mgh.harvard.edu/primerbank/index.html) or designed with the Primer3 tool (https://bioinfo.ut.ee/primer3).[36] GAPDH was used as the housekeeping gene. The sequences and IDs of the primers used are listed in Table 1.

Statistical Analysis. Data related to the viability assay are the mean ± SD of three separate experiments. For each experimental time, results are expressed as the percentage of the values obtained in the corresponding control cells set equal to 100%. Differences between group means were assessed by analysis of variance followed by the *post hoc* Newman−Keuls test. Data related to the gene expression are the mean of two separate experiments.

Table 1. Sequences and IDs of the Primers Used for the Experiments[a,b]

gene	primer ID	sequence
IL-10	24430216c1	F 5′-GAC TTT AAG GGT TAC CTG GGT TG-3′
		R 5′-TCA CAT GCG CCT TGA TGT CTG-3′
GAPDH		F 5′-CGG GAA ACT GTG GCG TGA TG-3′
		R 5′-ATG CCA GTG AGC TTC CCG TT-3′

[a]Each Sample Was Tested in Duplicate with the Quantitation Cycle (Cq) Values Averaged. [b]Each sample was tested in duplicate with the quantitation cycle (Cq) values averaged. The relative mRNA amount was calculated with the $2^{-\Delta\Delta Cq}$ method, where $\Delta Cq = Cq_{sample} - Cq_{GAPDH}$ and $\Delta\Delta Cq = \Delta Cq_{treatment} - \Delta Cq_{control}$.

RESULTS AND DISCUSSION

Synthesis

In the recent past, a procedure to prepare conjugates of hyaluronan with natural fatty acids was performed via mechanical milling of the polysaccharide with the anhydrides of oleic, linoleic, and palmitic acids, in the presence of K_2CO_3.[5,20] The MW irradiation was employed to activate the esterification process, since the radiation was very efficiently and directly adsorbed by polar/ionic compounds, thus generating a molecule-focused heating. Starting from these experimental conditions, a MW-assisted protocol to conjugate CUR to HA was developed.

As shown in Scheme 1, the synthesis of our conjugates was carried out by esterification of the hyaluronan carboxylic functions with the CUR hydroxyl groups. This strategy required that first, the hyaluronan carboxylic functions were activated, and this was obtained via the *N,N′*-diisopropylcarbodiimide (DIC) coupling protocol.

The reaction was performed in the absence of any solvent and in the presence of an organic base such as 4-dimethylaminopyridine (DMAP) (Steglich conditions)[37] or an inorganic base (K_2CO_3). In addition, the activation was also performed in the absence of any base (Scheme 1). All reactants were finely milled by an agate mortar, and then, the mixture was placed into a specific MW reaction vessel. The solid-state reaction was activated by microwave radiation while the temperature was left at the fixed value of 80 °C. Then, different reaction times were explored until we come up to a reliable and reproducible protocol. In particular, conditions of entry B (80 °C and 2 min for both activation and esterification steps) were selected as conditions of entry A were characterized by a low degree of functionalization, while it is likely that conditions of entry C triggered some degradations of both molecules (Table 2).

It is worth remembering that the activation−esterification protocol employing DMAP is reported as very effective, even in the absence of any solvent.[38,39] In major detail, DMAP

Table 2. Microwave Reaction Times for the Synthetic Steps to Prepare HA-CUR Conjugates

entry	temperature (°C)	activation (min)	esterification (min)
A	80	1	2
B	80	2	2
C	80	3	2

https://doi.org/10.1021/acspolymersau.3c00047
ACS Polym. Au 2024, 4, 214−221

activates the carboxylic function, thanks to its great nucleophilicity, by reacting with the *O*-acylisourea intermediate to form the acylated pyridinium ion (Route 1), as electrophilic species are very sensitive to promptly react with the alcoholic function of CUR. On the other hand, the activation of the hyaluronan carboxylic functions as *O*-acylisourea species was obtained in the presence of K_2CO_3 (Route 2) or in the absence of base (Route 3). Concerning these derivatives, they are quite unstable and can easily decompose or rearrange to stable *N*-acylisourea when dissolved in a liquid solvent. In our case, a solvent-free reaction is performed, and due to their lower polarity, these activated intermediates are less sensitive to the "heating" produced by MW radiation. These conditions are a key factor for the success of our protocol.

The validation of the activation step could only be provided by the subsequent esterification, which was performed by CUR hydroxyl groups. The same MW instrumental conditions employed to conjugate fatty acids to HA were set up. The solid reactants were mechanically milled and transferred into the MW reactor to be irradiated at T = 80 °C for 2 min (step B of Scheme 1).

Structural Characterization

The FT-IR spectra of HA−CUR conjugates are shown in Figure 1, and for comparison purposes, a spectrum of native HA is also included. The chemical modification of the HA produced a main change of the spectrum, i.e., a new band in the C═O ester stretching region (1730 cm^{-1}) appeared. It accounted for the esterification of the hyaluronan carboxylic functions with the hydroxyl groups of CUR. Concerning the band at 1639 cm^{-1}, it featured stretching of the HA carboxylic function. The reduction of its intensity in the HA-CUR spectra could be ascribed to the esterification process (Figure 1, Panel B). Finally, the characteristic bands around 1000 cm^{-1} were typical of skeletal HA stretching and also of the aromatic structure of CUR. FT-IR spectra allowed us to conclude that the esterification was efficiently performed by following all activation protocols.

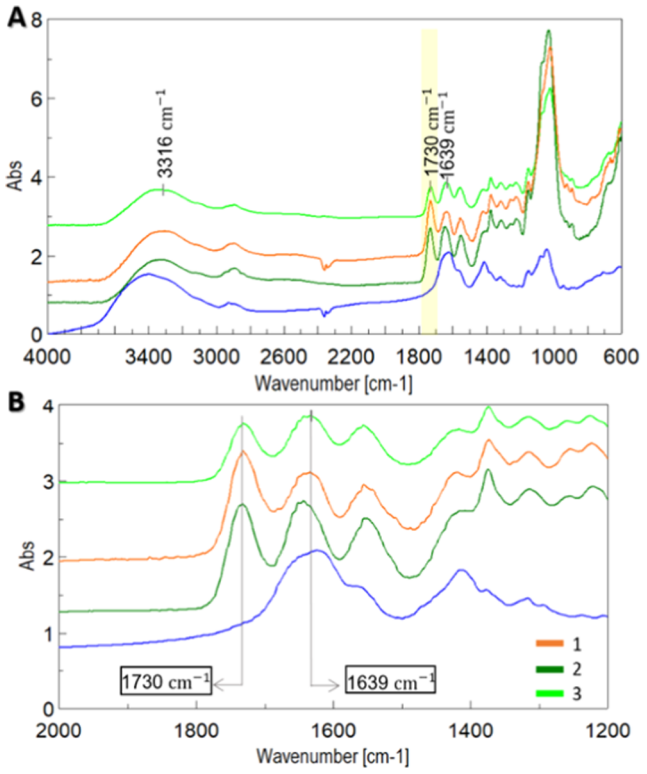

Figure 1. FT-IR spectra of HA (blue) and HA-CUR conjugates obtained by activation with DMAP (dark green) and K_2CO_3 (orange) or in absence of any base (light green) (A) and expansion of HA-CUR FT-IR spectra (B).

HA-CUR conjugates were investigated also by ^{1}H NMR analysis in D_2O and in 3:2 v/v DMSO-d_6−D_2O. The spectra measured in D_2O showed only the typical signals associated with the HA backbone (at 4.6−3.3 ppm) and the acetamido functionality (at 2.0 ppm) decorating the aminosugar residues, while no significant signals could be detected in the aromatic region (7.7−6.7 ppm) typical for the curcumin moiety (Figures S1 and S2, Supporting Information). Conversely, the ^{1}H NMR spectrum measured in 3:2 v/v DMSO-d_6−D_2O showed the presence of both HA polysaccharide (at 4.6−3.0 and 1.8 ppm) and curcumin signals (at 7.5−6.5 ppm). Noteworthily, the latter was clearly detectable also in a diffusion-ordered (1D-DOSY) spectrum (Figure 2), which is usually employed to distinguish between signals associated with low-molecular weight contaminants, typically faster self-diffusing in solution, and the cut off in the 1D-DOSY spectrum, and peaks related to slowly diffusing macromolecules.[40] Therefore, the presence of curcumin signals in the 1D-DOSY spectrum demonstrated the covalent conjugation of curcumin moieties to the HA backbone. Furthermore, the low intensity characterizing the curcumin signals could be due to the amphiphilic nature of HA-CUR, exposing the polysaccharide backbone toward the solvent (D_2O or 3:2 v/v DMSO-d_6−D_2O), while the apolar moieties of the curcumin are likely embedded in the inner core of a macromolecular aggregate structure and therefore not present at all or not highly intense in D_2O or 3:2 v/v DMSO-d_6−D_2O NMR spectra, respectively.

Therefore, for a more accurate evaluation of the curcumin content in HA-CUR conjugates, UV−vis absorption spectroscopy was employed to estimate the curcumin concentration in each conjugate obtained using the different synthetic conditions (routes 1, 2, and 3 in Scheme 1). This determination was mandatory for the subsequent biological tests. UV−visible and fluorescence spectroscopies have been mostly used to characterize the integrity of CUR in the water/ethanol (EtOH) solvent system.[41−43] It was reported that a prominent band at 429 nm, related to the tautomeric keto−enol form, together with a weaker band at 350 nm, related to the diketo tautomer, is observed upon registration of UV−vis spectra of CUR dissolved in water containing a certain percentage of EtOH. An increase of the peak intensity at 429 nm and a gradually concomitant reduction of that at 350 nm are observed in the presence of a high percentage of EtOH.[41] As shown in Figure 3, UV−vis of our HA-CUR conjugates resulted very similar to that of pristine CUR, having acquired both in the same solvent system (3:2 v/v EtOH−H_2O).

By using the equation of Lambert−Beer (eq 1), the concentration of CUR (C) in the HA-CUR conjugates was determined (Table 3). In particular, an amount of HA-CUR (m) lower than 1.0 mg was dissolved in 10 mL of the solvent system, and the absorption intensity (Abs) at λ_{max} = 432 nm (ε = 51,818 M^{-1} cm^{-1}) was measured. In addition, we could also estimate through eq 2 the degree of substitution (DS), i.e., the average amount of carboxylic acid effectively functionalized as CUR ester conjugates per HA repeating unit.

https://doi.org/10.1021/acspolymersau.3c00047
ACS Polym. Au 2024, 4, 214−221

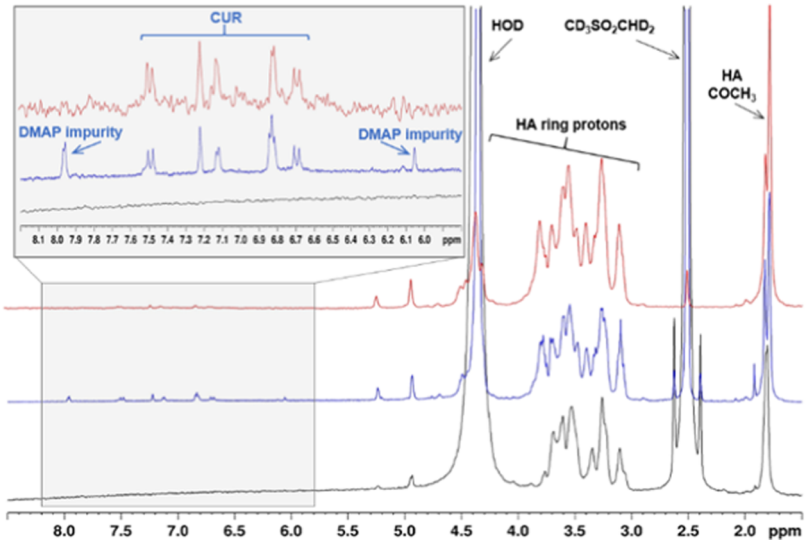

Figure 2. ^{1}H NMR spectra (600 MHz, 298 K, 3:2 v/v DMSO-d_6–D_2O) of HA (black) and HA-CUR (blue) and 1D-DOSY NMR spectrum (red) of the latter.

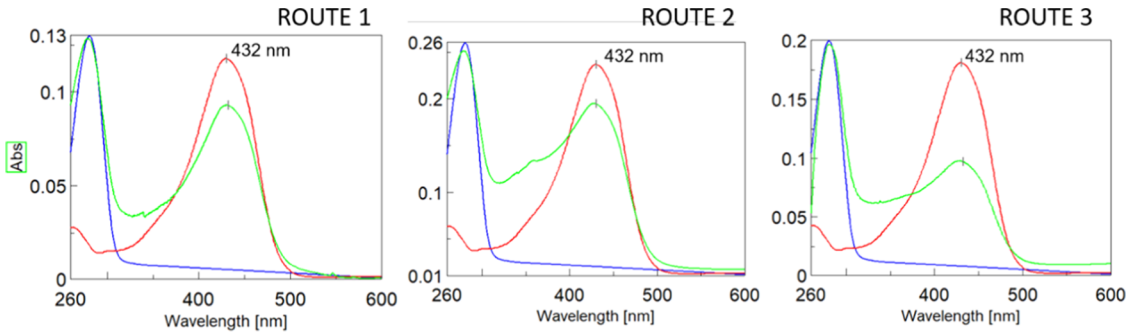

Figure 3. UV–vis normalized spectra in 3:2 v/v EtOH–H_2O of HA (blue), CUR (red), and HA-CUR conjugates (light green) obtained with three synthetic strategies (see Scheme 1).

Table 3. DS of HA-CUR Conjugates Obtained with Three Different Synthetic Strategies (see Scheme 1)

entry (route)	Abs_{432}	m [mg]	C [mM]	DS[a]
route 1-DMAP	0.09259	0.50	0.00178	0.026
route 2-K_2CO_3	0.08890	0.30	0.00171	0.042
route 3-no base	0.19331	0.70	0.00373	0.0096

[a]Calculated by applying eq 2 with M_W = HA-CUR repeating unit molecular weight = 729.67 g mol^{-1}

$$C = \frac{\text{Abs}}{\varepsilon} \times 1000 \quad (1)$$

$$\text{DS} = \frac{C}{\frac{(m / \text{MW}) \times 1000}{10}} \quad (2)$$

To further gain insights into the chemical structure of the CUR covalently bound to hyaluronan, we registered fluorescence spectra of HA-CUR and pristine CUR in the same solvent system (3:2 v/v EtOH–H_2O). The obtained results revealed that the behavior of both compounds totally matches the same characteristic emission spectrum upon excitation at the same wavelength (430 nm) (Figure 4).

These results assessed that the hotspot solid-state esterification process is fully successful by using all the exploited activation procedures (1, 2, and 3), which means that the employment of a hazardous substance, such as DMAP, to accelerate the reaction can be avoided.

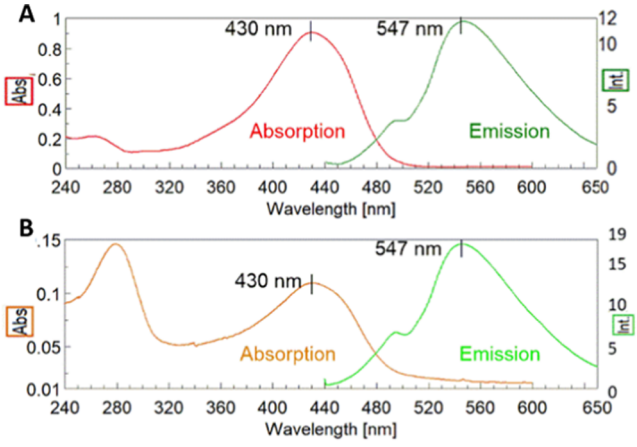

Figure 4. Absorption and fluorescence emission spectra (λ_{exc} = 430 nm) of CUR (A) and HA-CUR (B) in 3:2 v/v EtOH–H_2O.

Biological Evaluation

The biocompatibility of a HA-CUR conjugate was investigated using an MTT assay that evaluates the mitochondrial metabolic activity and therefore is considered a good indicator of cell viability. We selected route 2 (see Scheme 1) to prepare

https://doi.org/10.1021/acspolymersau.3c00047
ACS Polym. Au 2024, 4, 214–221

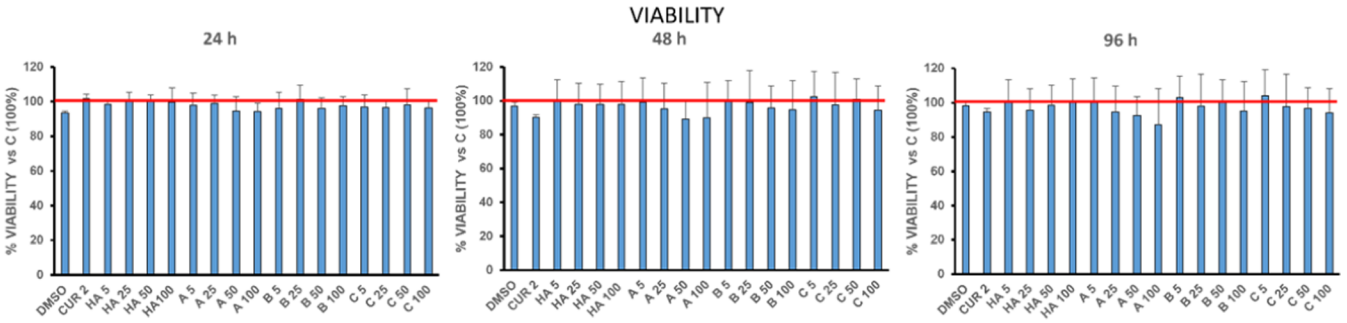

Figure 5. Viability of the human fibroblast cell line HFF-1 exposed to (from left to right): DMSO 0.55%, CUR 2 μg/mL; HA 5, 25, 50, and 100 μg/mL; and HA-CUR conjugates (A, B, and C) 5, 25, 50, and 100 μg/mL.

three independent samples (named A, B, and C), since this route ensured the highest content of CUR conjugation to HA.

The results reported in Figure 5 evidenced no significant reduction of viability of HFF-1 fibroblasts at various concentrations of HA-CUR as a function of the experimental time.

Moreover, the morphological analysis of treated cells evidenced no changes in comparison with untreated ones (Figure S4, Supporting Information). In addition, no detached cells (corresponding to dead cells) were present in the culture medium (data not shown), which confirmed the high biocompatibility of the developed HA-CUR conjugate. Besides the *in vitro* cytotoxicity test, preliminary experiments were performed to evaluate the bioactivity of the HA-CUR conjugate as an anti-inflammatory agent. It is reported that HA, as a signaling molecule, can exert opposing actions, such as pro- or anti-inflammatory effects, depending above all on its molecular weight.[44] On the other side, CUR binds several receptors, interfering with the expression of several factors; among them, CUR is able to upregulate interleukin-10 (IL-10), a well-known anti-inflammatory molecule.[32] Therefore, we investigated the expression of IL-10 in human cultured fibroblasts HFF-1, upon treatment with the HA-CUR conjugate. For this purpose, the real-time PCR technique was employed. The results (Figure 6) confirmed that HA-CUR is able to increase (2.5- or 1.6-fold, respectively) the IL-10 mRNA content when compared with that of cells untreated or treated with the native HA polysaccharide alone. These preliminary results are a good indicator for designing further anti-inflammatory studies of the HA-CUR conjugate.

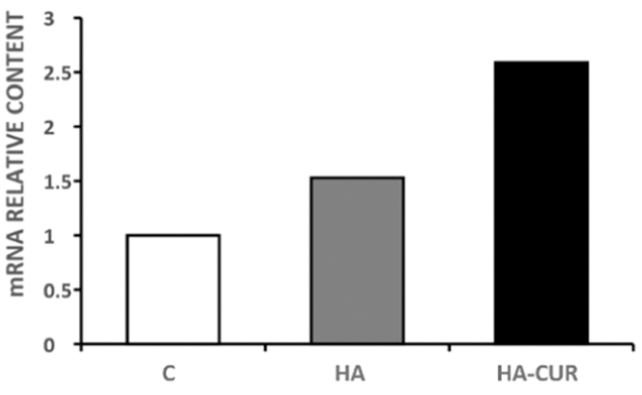

Figure 6. Interleukin-10 (IL-10) expression in human fibroblasts HFF-1 after 96 h of treatment (C, untreated cells; HA 100 μg/mL; and HA-CUR conjugate 100 μg/mL). Data represent the mean of two independent experiments.

CONCLUSIONS

A new synthetic strategy to conjugate CUR to HA using a solvent-free protocol was developed. It consists of an effective microwave-promoted, solid-state acylation of the hydroxyl function of CUR with the carboxylic groups of hyaluronic acid, which were previously activated by carbodiimide chemistry. The novelty of the protocol consists of performing each step of the reaction in the absence of any solvent. Even the activation of the hyaluronan carboxylic groups was a MW-promoted, solid-state synthetic step performed on the same molecule and in the absence of DMAP, which, to the best of our knowledge, is an unexplored chemical process until now for HA.[45] The great advantage of totally eliminating the use of organic solvents and a toxic reagent, such as DMAP, along with a very short activation time performed by MW radiation, makes the conjugation strategy even more ecocompatible in terms of chemical and energy consumption. In addition, the reaction conditions allowed us to preserve the integrity of a sensitive molecule, such as CUR, as proven by the spectroscopic characterization performed on the obtained HA-CUR conjugate. The biocompatibility studies evidenced that the HA-CUR conjugate does not induce any significant decrease of the human fibroblast viability, which is a fundamental requirement for the implementation of the newly developed material for healthcare applications. In addition, the higher expression of the anti-inflammatory molecule IL-10 found for HA-CUR-treated human fibroblasts suggests that the conjugate is endowed with a good bioactivity that deserves further investigation.

ASSOCIATED CONTENT

Supporting Information

The Supporting Information is available free of charge at https://pubs.acs.org/doi/10.1021/acspolymersau.3c00047.

Additional figures of morphological analyses and NMR spectra and NMR chemical shift of compounds (PDF)

AUTHOR INFORMATION

Corresponding Author

Stefania De Luca − *Institute of Biostructures and Bioimaging, National Research Council, 80131 Naples, Italy;*
orcid.org/0000-0002-7078-1696;
Email: stefania.deluca@cnr.it

https://doi.org/10.1021/acspolymersau.3c00047
ACS Polym. Au 2024, 4, 214−221

Authors

Valentina Verdoliva − *Institute of Biostructures and Bioimaging, National Research Council, 80131 Naples, Italy*
Giuliana Muzio − *Department of Clinical and Biological Sciences, University of Turin, 10125 Turin, Italy*
Riccardo Autelli − *Department of Clinical and Biological Sciences, University of Turin, 10125 Turin, Italy*
Michele Saviano − *Institute of Crystallography, National Research Council, 81100 Caserta, Italy*
Emiliano Bedini − *Department of Chemical Sciences, University of Naples Federico II, 80126 Naples, Italy;* orcid.org/0000-0003-4923-3756

Complete contact information is available at: https://pubs.acs.org/10.1021/acspolymersau.3c00047

Author Contributions

V.V.: data curation, investigation, methodology (synthesis, UV−vis, fluorescence), software, and writing—original draft. **G.M.**: data curation, investigation, methodology (biological test), and writing—original draft. **R.A.**: data curation, investigation, methodology (biological test), and writing—original draft. **M.S.**: data curation, funding acquisition, and writing—original draft. **E.B.**: data curation, funding acquisition, methodology (NMR spectroscopy), validation, and writing—review and editing. **S.D.L.:** conceptualization, investigation, methodology (synthesis, UV−vis, fluorescence), project administration, supervision and validation, writing—original draft, and writing—review and editing.

Notes

The authors declare no competing financial interest.

■ ACKNOWLEDGMENTS

The authors thank Leopoldo Zona, Luca De Luca, and Maurizio Amendola for the technical assistance. This work was supported by Italian Ministry for University and Research (MUR) [grant PRIN2022-PNR_P20224T45H to EB], and by National Research Council of Italy (Cnr) ["The Bioinorganic Drugs (BIDs) joint laboratory: A multidisciplinary platform promoting new molecular targets for drug discovery" to MS].

■ REFERENCES

(1) Abdussalam-Mohammed, W.; Ali, A. Q.; Errayes, A. O. Green chemistry: Principles, applications, and disadvantages. *Chem. Methodol.* **2020**, *4*, 408−423.
(2) Anastas, P.; Eghbali, N. Green chemistry: Principles and practice. *Chem. Soc. Rev.* **2010**, *39*, 301−312.
(3) Manchala, S.; Tandava, V. S. R. K.; Jampaiah, D.; Bhargava, S. K.; Shanker, V. Novel and highly efficient strategy for the green synthesis of soluble graphene by aqueous polyphenol extracts of eucalyptus bark and its applications in high-performance supercapacitors. *ACS Sustainable Chem. Eng.* **2019**, *7*, 11612−11620.
(4) Zimmerman, J. B.; Anastas, P. T.; Erythropel, H. C.; Leitner, W. Designing for a green chemistry future. *Science* **2020**, *367*, 397−400.
(5) Calce, E.; Mercurio, F. A.; Leone, M.; Saviano, M.; De Luca, S. Eco-friendly microwave-assisted protocol to prepare hyaluronan-fatty acid conjugates and to induce their self-assembly process. *Carbohydr. Polym.* **2016**, *143*, 84−89.
(6) Calce, E.; Petricci, E.; Saviano, M.; De Luca, S. Green microwave-assisted procedure to generate bio-based pectin materials. *Sustainable Chem. Pharm.* **2017**, *5*, 127−130.
(7) Seo, T.; Toyoshima, N.; Kubota, K.; Ito, H. Tackling solubility issues in organic synthesis: Solid-state cross-coupling of insoluble aryl halides. *J. Am. Chem. Soc.* **2021**, *143*, 6165−6175.
(8) Agrawal, N.; Jaiswal, M. Bioavailability enhancement of curcumin via esterification processes: A review. *Eur. J. Med. Chem.* **2022**, *6*, No. 100081.
(9) Boroumand, N.; Samarghandian, S.; Hashemy, S. I. Immunomodulatory, anti-inflammatory, and antioxidant effects of curcumin. *J. HerbMed Pharmacol.* **2018**, *7*, 211−219.
(10) Ghosh, S.; Banerjee, S.; Sil, P. C. The beneficial role of curcumin on inflammation, diabetes and neurodegenerative disease: A recent update. *Food Chem. Toxicol.* **2015**, *83*, 111−124.
(11) Noorafshan, A.; Ashkani-Esfahani, S. A review of therapeutic effects of curcumin. *Curr. Pharm. Des.* **2013**, *19*, 2032−2046.
(12) Shentu, C.-Y.; Yan, G.; Xu, D.-C.; Chen, Y.; Peng, L.-H. Emerging pharmaceutical therapeutics and delivery technologies for osteoarthritis therapy. *Front. Pharmacol.* **2022**, *13*, No. 945876.
(13) Sethiya, A.; Agarwal, D. K.; Agarwal, S. Current Trends in Drug Delivery System of Curcumin and its Therapeutic Applications. *Mini Rev Med Chem.* **2020**, *20* (13), 1190−1232.
(14) Kumavat, S. D.; Chaudhari, Y. S.; Borole, P.; Mishra, P.; Shenghani, K.; Duvvuri, P. Degradation studies of curcumin. *Int. J. Pharm. Rev. Res.* **2013**, *3*, 50−55.
(15) Lopresti, A. L. The problem of curcumin and its bioavailability: could its gastrointestinal influence contribute to its overall health-enhancing effects? *Adv. Nutr.* **2018**, *9*, 41−50.
(16) Wang, Y.-J.; Pan, M.-H.; Cheng, A.-L.; Lin, L.-I.; Ho, Y.-S.; Hsieh, C.-Y.; Lin, J.-K. Stability of curcumin in buffer solutions and characterization of its degradation products. *J. Pharm. Biomed. Anal.* **1997**, *15*, 1867−1876.
(17) Cheng, K. K.; Yeung, C. F.; Ho, S. W.; Chow, S. F.; Chow, A. H.; Baum, L. Highly stabilized curcumin nanoparticles tested in an in vitro blood-brain barrier model and in Alzheimer's disease Tg2576 mice. *AAPS J.* **2013**, *15*, 324−336.
(18) Cho, H. J.; Yoon, H. Y.; Koo, H.; Ko, S. H.; Shim, J. S.; Lee, J. H.; Kim, K.; Kwon, I. C.; Kim, D. D. Self-assembled nanoparticles based on hyaluronic acid-ceramide (HA-CE) and Pluronic for tumor-targeted delivery of docetaxel. *Biomaterials* **2011**, *32*, 7181−7190.
(19) Del Prado-Audelo, M. L.; Magaña, J. J.; Mejía-Contreras, B. A.; Borbolla-Jiménez, F. V.; Giraldo-Gomez, D. M.; Piña-Barba, M. C.; Quintanar-Guerrero, D.; Leyva-Gómez, G. In vitro cell uptake evaluation of curcumin-loaded PCL/F68 nanoparticles for potential application in neuronal diseases. *J. Drug Delivery Sci. Technol.* **2019**, *52*, 905−914.
(20) Pepe, G.; Calce, E.; Verdoliva, V.; Saviano, M.; Maglione, V.; Di Pardo, A.; De Luca, S. Curcumin-loaded nanoparticles based on amphiphilic hyaluronan-conjugate explored as targeting delivery system for neurodegenerative disorders. *Int. J. Mol. Sci.* **2020**, *21*, 8846.
(21) Tiwari, S. K.; Agarwal, S.; Seth, B.; Yadav, A.; Nair, S.; Bhatnagar, P.; Karmakar, M.; Kumari, M.; Chauhan, L. K.; Patel, D. K.; et al. Curcumin-loaded nanoparticles potently induce adult neurogenesis and reverse cognitive deficits in Alzheimer's disease model via canonical Wnt/-catenin pathway. *ACS Nano* **2014**, *8*, 76−103.
(22) Tsai, Y. M.; Chien, C. F.; Lin, L. C.; Tsai, T. H. Curcumin and its nano-formulation: The kinetics of tissue distribution and blood−brain barrier penetration. *Int. J. Pharmacol.* **2011**, *416*, 331−338.
(23) Ali, P.; Kirmani, S. A. K.; Rugaie, O. A.; Azam, F. Degree-based topological indices and polynomials of hyaluronic acid-curcumin conjugates. *Saudi Pharm. J.* **2020**, *28*, 1093−1100.
(24) Charan, T. R.; Bhutto, M. A.; Bhutto, M. A.; Tunio, A. A.; Khuhro, G. M.; Khaskheli, S. A.; Mughal, A. A. Nanomaterials of curcumin-hyaluronic acid": Their various methods of formulations, clinical and therapeutic applications, present gap, and future directions. *Future J. Pharm. Sci.* **2021**, *7*, No. 126.
(25) Fan, Z.; Li, J.; Liu, J.; Jiao, H.; Liu, B. Anti-inflammation and joint lubrication dual effects of a novel hyaluronic acid/curcumin nanomicelle improve the efficacy of rheumatoid arthritis therapy. *ACS Appl. Mater. Interfaces* **2018**, *10*, 23595−23604.

(26) Mudagal, M. P.; Janadri, S. Curcumin on to hyaluronic acid conjugate enhance cytotoxicity. *Asian J. Pharm. Pharmacol.* **2019**, *5*, 281−285.
(27) Mudagal, M. P.; Janadri, S.; Taj, N. In-vivo anticancer activity of curcumin-hyaluronic acid conjugate. *Adv. Pharm. J.* **2019**, *4*, 85−89.
(28) Sharma, M.; Sahu, K.; Singh, S. P.; Jain, B. Wound healing activity of curcumin conjugated to hyaluronic acid: In vitro and in vivo evaluation. *Artif. Cells, Nanomed., Biotechnol.* **2018**, *46*, 1009−1010.
(29) Yu, D.; Zhuang, Z.; Ren, J.; Hu, X.; Wang, Z.; Zhang, J.; Luo, Y.; Wang, K.; He, R.; Wang, Y. Hyaluronic acid-curcumin conjugate suppresses the fibrotic functions of myofibroblasts from contractive joint by the PTGER2 demethylation. *Regener. Biomater.* **2019**, *6*, 269−277.
(30) Dubashynskaya, N. V.; Bokatyi, A. N.; Gasilova, E. R.; Dobrodumov, A. V.; Dubrovskii, Y. A.; Knyazeva, E. S.; Nashchekina, Y. A.; Demyanova, E. V.; Skorik, Y. A. Hyaluronan-colistin conjugates: Synthesis, characterization, and prospects for medical applications. *Int. J. Biol. Macromol.* **2022**, *215*, 243−252.
(31) Mitsui, Y.; Gotoh, M.; Nakama, K.; Yamada, T.; Higuchi, F.; Nagata, K. Hyaluronic acid inhibits mRNA expression of proinflammatory cytokines and cyclooxygenase-2/prostaglandin E_2 production via CD44 in interleukin-1-stimulated subacromial synovial fibroblasts from patients with rotator cuff disease. *J. Orthop. Res.* **2008**, *26*, 1032−1037.
(32) Peng, Y.; Ao, M.; Dong, B.; Jiang, Y.; Yu, L.; Chen, Z.; Hu, C.; Xu, R. Anti-inflammatory effects of curcumin in the inflammatory diseases: Status, limitations and countermeasures. *Drug Des., Dev. Ther.* **2021**, *15*, 4503−4525.
(33) Rooney, P.; Srivastava, A.; Watson, L.; Quinlan, L. R.; Pandit, A. Hyaluronic acid decreases IL-6 and IL-8 secretion and permeability in an inflammatory model of interstitial cystitis. *Acta Biomater.* **2015**, *19*, 66−75.
(34) Tiwari, S.; Bahadur, P. Modified hyaluronic acid based materials for biomedical applications. *Int. J. Biol. Macromol.* **2019**, *121*, 556−571.
(35) Majhi, A.; Rahman, G. M.; Panchal, S.; Das, J. Binding of curcumin and its long chain derivatives to the activator binding domain of novel protein kinase C. *Bioorg. Med. Chem.* **2010**, *18*, 1591−1598.
(36) Wang, X.; Spandidos, A.; Wang, H.; Seed, B. PrimerBank: A PCR primer database for quantitative gene expression analysis, 2012 update. *Nucleic Acids Res.* **2012**, *40*, D1144−D1149.
(37) Zhang, J.; Zheng, Y.; Luo, Y.; Du, Y.; Zhang, X.; Fu, J. Curcumin inhibits LPS-induced neuroinflammation by promoting microglial M2 polarization via TREM2/TLR4/NF-κB pathways in BV2 cells. *Mol. Immunol.* **2019**, *116*, 29−37.
(38) Traboni, S.; Esposito, F.; Ziaco, M.; Bedini, E.; Iadonisi, A. A comprehensive solvent-free approach for the esterification and amidation of carboxylic acids mediated by carbodiimides. *Tetrahedron* **2023**, *133*, No. 133291.
(39) Traboni, S.; Bedini, E.; Vessella, G.; Iadonisi, A. Solvent-free approaches in carbohydrate synthetic chemistry: Role of catalysis in reactivity and selectivity. *Catalysts* **2020**, *10*, 1142.
(40) Bedini, E.; Cassese, E.; D'Agostino, A.; Cammarota, M.; Frezza, M. A.; Lepore, M.; Portaccio, M.; Schiraldi, C.; La Gatta, A. Self-esterified hyaluronan hydrogels: Advancements in the production with positive implications in tissue healing. *Int. J. Biol. Macromol.* **2023**, *236*, No. 123873.
(41) Bhatia, N. K.; Kishor, S.; Katyal, N.; Gogoi, P.; Narang, P.; Deep, S. Effect of pH and temperature on conformational equilibria and aggregation behaviour of curcumin in aqueous binary mixtures of ethanol. *RSC Adv.* **2016**, *6*, 103275−103288.
(42) Ali, Z.; Saleem, M.; Atta, B. M.; Khan, S. S.; Hammad, G. Determination of curcuminoid content in turmeric using fluorescence spectroscopy. *Spectrochim. Acta, Part A* **2019**, *213*, 192−198.
(43) Mondal, S.; Ghosh, S.; Moulik, S. P. Stability of curcumin in different solvent and solution media: UV−visible steady-state fluorescence spectral study. *J. Photochem. Photobiol., B* **2016**, *158*, 212−218.
(44) Marinho, A.; Nunes, C.; Reis, S. Hyaluronic acid: A key ingredient in the therapy of inflammation. *Biomolecules* **2021**, *11*, 1518.
(45) Hintze, V.; Schnabelrauch, M.; Rother, S. Chemical modification of hyaluronan and their biomedical applications. *Front. Chem.* **2022**, *10*, No. 830671.

https://doi.org/10.1021/acspolymersau.3c00047
ACS Polym. Au 2024, 4, 214−221